Operation Characteristics of Diverging Magnetic Field Electrostatic Thruster

IEPC-2017-193

Presented at the 35th International Electric Propulsion Conference
Georgia Institute of Technology • Atlanta, Georgia • USA
October 8 – 12, 2017

Daisuke Ichihara[1], Akira Iwakawa[2] and Akihiro Sasoh[3]
Nagoya University, Nagoya, Aichi, 464-8603, Japan

Abstract: Operation characteristics of diverging magnetic field electrostatic thruster (DM-EST) that has a diverging magnetic field applied by solenoid coil in the ion acceleration region, which comprised a ring anode in upstream region and off-axis hollow cathode in downstream region. By increasing the strength of magnetic field near the ring anode, injected propellant was fully ionized and obtained kinetic energy of 79% of discharge energy. Based on these results, permanent magnet used DM-EST was developed and demonstrated 22% of thrust efficiency at 2700 sec of specific impulse.

Nomenclature

E_i	=	ion beam energy
F	=	thrust
I_{sp}	=	specific impulse
$\hat{J}_1$	=	propellant flow rate through the annular slit in current equivalent
$\hat{J}_2$	=	propellant flow rate through the hollow cathode in current equivalent
J_d	=	discharge current
J_i	=	total ion beam current
J_k	=	keeper current
r, z	=	cylindrical coordinates
V_d	=	discharge voltage
V_k	=	keeper voltage
η	=	thrust efficiency
θ	=	half-beam divergence angle

I. Introduction

Mitigating collisions between electrostatically accelerated ions and discharge channel wall is one of the most important challenge to extend the life-time of electric propulsion. In an ion thruster, acceleration grids are designed based on ion trajectory calculation[1]. In a stationary-plasma-thruster (SPT)-type Hall thruster, intensive investigation were performed such as "magnetic shielding[2]" and "wall-less Hall thruster[3]". Cylindrical Hall thrusters[4], high efficiency multistage plasma thrusters[5], and cusped-field thrusters[6] have a cusped magnetic field in order to accelerate ions apart from the discharge channel wall. Harada et al[7] demonstrated electrostatic ion acceleration by combining a cusped magnetic field with ring anode and hollow cathode. We inspired by this result and proposed the diverging magnetic field electrostatic thruster (DM-EST)[8]. For utilizing applied voltage to accelerate ions efficiently, generating ions near the anode potential region is important. In ref. 8 we reported that by injecting the working gas

[1] Research associate, Department of Aerospace Engineering, ichihara@fuji.nuae.nagoya-u.ac.jp.
[2] Lecturer, Department of Aerospace Engineering, iwakawa@nuae.nagoya-u.ac.jp.
[3] Professor, Department of Aerospace Engineering, sasoh@nuae.nagoya-u.ac.jp.

only from the ring anode inner surface, both ionization and electrostatic acceleration performances were enhanced. In this paper, magnetic field profile effects on the ion generation and electrostatic acceleration are investigated.

II. Experimental apparatus

Figure 1 shows a schematic of the nominal condition of DM-EST. The primary components such as solenoid coil, ring anode and the hollow cathode and insulating channel walls were same as these of HEST[7]. An insulating plate fabricated using boron nitride was located inside the ring anode. The propellant, argon, was injected through the 1.5-mm-thick annular slit between the inner surface of the ring anode and the insulating plate. The orifice of the hollow cathode (DLHC-1000, Kaufman & Robinson, Inc.) was located at 70 mm off-axis and 175 mm downstream from the solenoid coil center.

In order to modify the magnetic field profile inside the ring anode, a ring yokes fabricated using soft iron were introduced. Figure 2 shows the two magnetic field profiles, types N and A. Here, the cylindrical coordinates (r, z) are defined on the central axis with their origin at the downstream surface of the insulating plate. The magnetic field type N was the same as that used in refs. 7 and 8. Type N has uniform magnetic field strength, that is, B(0 mm, 0 mm) = (13.5 mm, 0 mm) = 100 mT. In Type A, the insulating plate was backed by a copper inner support. By using yokes and outer support fabricated using soft iron, the magnetic field was strengthened near the ring anode inner surface, that is, B(0 mm, 0 mm) = 150 mT and B(13.5 mm, 0 mm) = 250 mT.

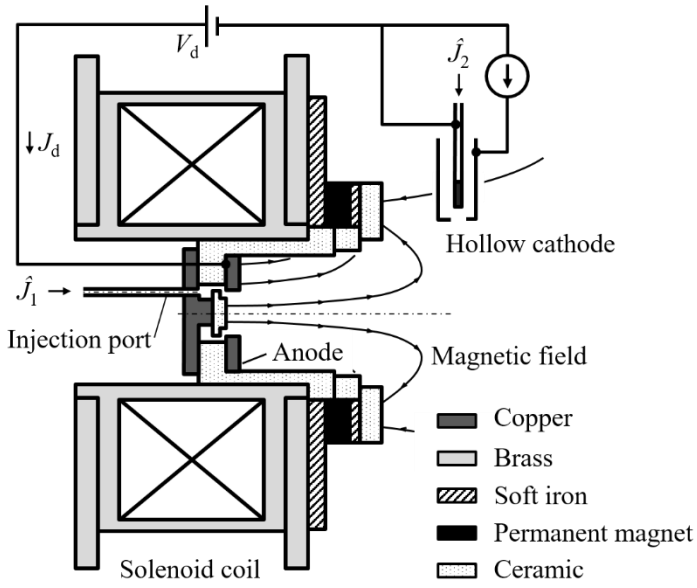

Figure 1. Schematic and electrical circuit of DM-EST, magnetic field type N.

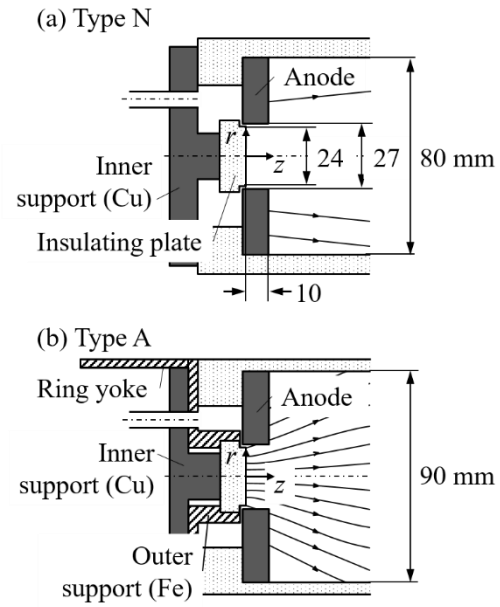

Figure 2. Applied-magnetic fields, (a) Type N, and (b)Type A.

Figure 3 shows a schematic of the DM-EST with flare-yoke. Type II has similar electromagnetic configurations. Yet, diverging magnetic field was applied by using Nd-FE-B permanent magnets and yokes. To make a diverging magnetic field, flare-shape yoke was used. The flare angle was set to 28 deg. The ring anode inner diameter was 27 mm. Propellant, argon, was injected through 1.5-mm-thick injection slit. The same hollow cathode as that of Type I thruster was located at 32 mm off-axis and 37 mm downstream from the downstream surface of the insulating plate.

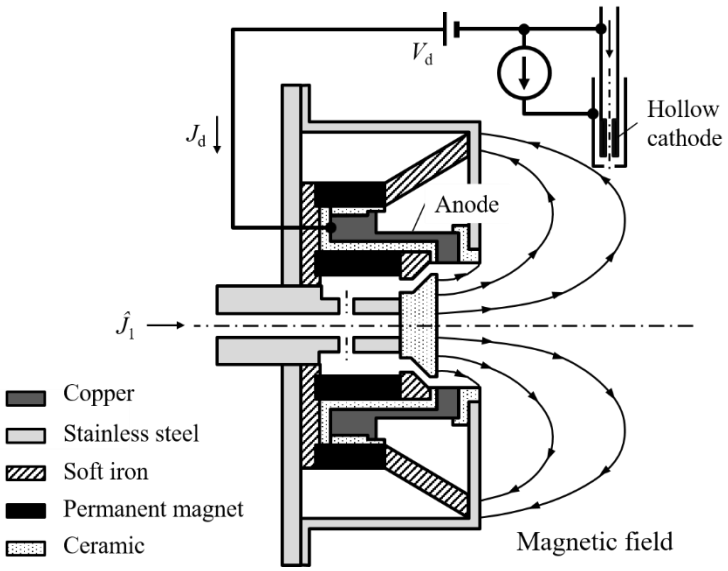

Figure 3. Schematic and electrical circuit of DM-EST with permanent magnets.

To evaluate the ion beam energy E_i from an ion energy distribution function (IEDF), a retarding potential analyzer (RPA) was used. The ion beam current J_i and half-beam divergence angle $\langle\theta\rangle$ were measured using a nude Faraday probe. Generated thrust F was measured by using gravitational pendulum type thrust stand. E_i, J_i, $\langle\theta\rangle$, and discharge current J_d measurements were conducted with Type I thruster. For thruster type II, F, and J_d were measured.

III. Experimental results

All experiments were conducted in a 3.2-m-long, 1.2-m-diameter stainless steel vacuum chamber. The propellant supplied through the slit and through the hollow cathode was argon (purity 99.9999%). The propellant flow rate through the slit, $\hat{J}_1$, was fixed to 1.0 Aeq for thruster Type I and varied from 2.0 Aeq to 4.0 Aeq for thruster Type II. Discharge voltage V_d ranged from 125 V to 300 V. The hollow cathode was operated with a propellant flow rate, $\hat{J}_2$, of 0.36 Aeq and keeper current of 2.0 A. Figure **4**(a) and (b) shows snapshots of thruster Type I and II in specific operating conditions, respectively.

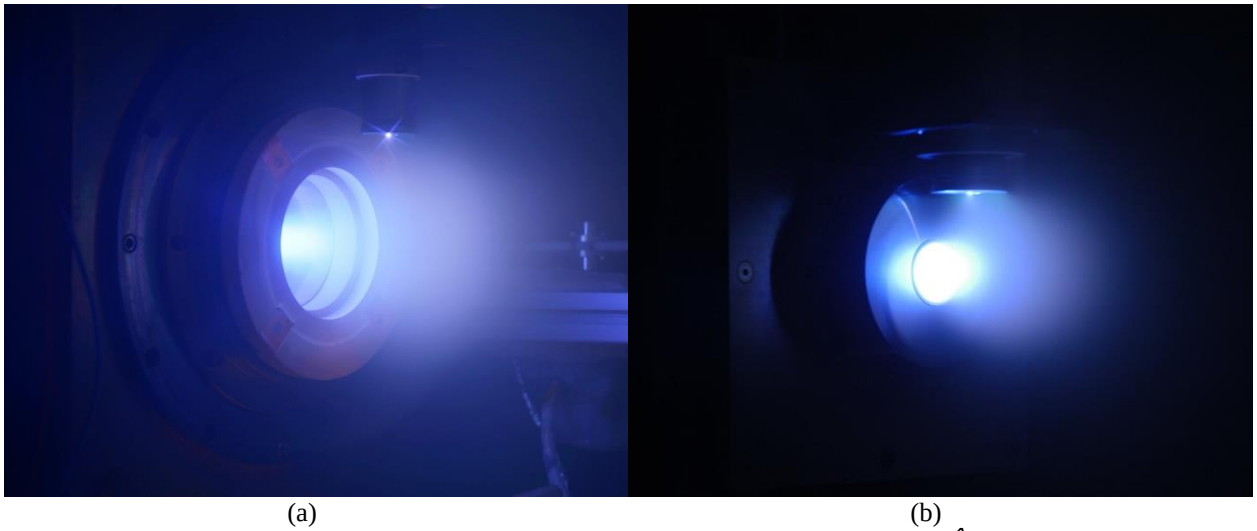

(a) (b)

Figure 4. Snapshot during experiment in specific conditions, (a) thruster Type I in $\hat{J}_1$ = 1.0 Aeq, V_d = 225 V and (b) thruster Type II in $\hat{J}_1$ = 3.0 Aeq, V_d = 275 V

Table 1 summarizes the ion generation and acceleration characteristics of Type I thruster. By applying Type N magnetic field, E_i and J_d increased linearly with increasing V_d. At V_d = 225 V operation, E_i/V_d equaled 0.59. $\langle\theta\rangle$ also showed increasing dependence on V_d.

Operation under Type A magnetic field showed another trend from Type N magnetic field operation. At V_d = 125 V operation, E_i was not calculated due to low signal-to-noise ratio. As increasing V_d, E_i increased linearly with the same increasing rate of $dE_i/dV_d \approx 1.0$. At V_d = 225 V, E_i/V_d reached 0.79. Ji increased with increasing V_d. However, J_i saturated at a value slightly higher than total injected propellant flow rate $\hat{J}_1 + \hat{J}_2$ (= 1.36 Aeq). J_d did not showed the saturation but increased linearly, up to 3 times higher than $\hat{J}_1$, with increasing V_d. $\langle\theta\rangle$ decreased with increasing V_d and saturated at about 39 deg. As shown in Fig. 2(b), increasing magnetic field strength near the ring anode enhanced the ion generation and electrostatic acceleration performance.

Table 1. Ion generation and acceleration characteristics of thruster Type I, $\hat{J}_1$ = 1.0 Aeq, $\hat{J}_2$ = 0.36 Aeq

Magnetic field type	V_d , V	E_i , eV	J_i , A	J_d , A	$\langle\theta\rangle$
N	175	99	0.79	1.77	49.7
	200	116	1.04	1.81	50.5
	225	132	1.11	2.12	52.3
A	125		0.87	1.79	42.0
	150	96	1.21	2.05	40.2
	175	123	1.36	2.26	39.2
	200	155	1.44	2.47	39.1
	225	178	1.49	2.72	39.2

Table 2 summarizes the operation characteristics of Type II thruster. Regardless of $\hat{J}_1$, both F and J_d increased as increasing V_d. Thrust efficiency η had a maximum value at $\hat{J}_1$ = 3.0 Aeq operation. Among the examined conditions, the maximum thrust efficiency was 22% with 2700 sec of specific impulse I_{sp}.

Table 2. Operation characteristics of thruster Type II, $\hat{J}_2$ = 0.36 Aeq

$\hat{J}_1$, Aeq	V_d , V	F , mN	J_d , A	I_{sp} , sec	η , %
2.0	150	7.9	2.6	819	7.4
	200	13.9	3.7	1443	12.7
	250	18.6	4.3	1932	15.9
	300	21.0	4.8	2187	15.4
3.0	250	31.0	7.4	2267	18.3
	275	34.2	7.5	2500	20.0
	300	37.8	7.6	2764	22.2
4.0	200	24.1	7.6	1355	10.3
	250	33.8	9.3	1900	13.4
	275	37.7	9.9	2123	14.3
	300	41.2	10.3	2321	15.0

IV. Conclusion

Operation characteristics of diverging magnetic field electrostatic thruster (DM-EST) was investigated. By increasing magnetic field strength near anode, both ion generation and electrostatic acceleration were enhanced, injected propellant gas was fully ionized and electrostatically accelerated up to 79% of applied voltage. Thrust efficiency of the permanent magnet type DM-EST had an optimal propellant flow rate. The maximum thrust efficiency reached 22% at 2700 sec of specific impulse.

Acknowledgments

This work was supported by JSPS KAKENHI (JP15H02321). The authors thanks to Akira Saitoh of the Technical Division, Nagoya University, for his technical supports.

References

[1] Michele Coletti and Stephen B. Gabriel, "The Application of Dual Stage Ion Optics to Ion Engines for High Power Missions," *IEEE Transactions on Plasma Science*, Vol. 40, No. 4, 2012, pp. 1053-1063.

[2] I. G. Mikellides, I. Katz, R. R. Hofer, and D. M. Goebel, "Magnetic shielding of a laboratory Hall thruster. I. theory and validation," *Journal of Applied Physics*, Vol. 115, 043303, 2014.

[3] S. Mazouffre, S. Tskikata, and J. Vaudolon, "Development and experimental characterization of a wall-less Hall thruster," *Journal of Applied Physics*, Vol. 116, 243302, 2014.

[4] K. D. Diamant, J. E. Pollard, Y. Raitses, and N. J. Fisch, "Ionization, plume properties, and performance of cylindrical Hall thrusters," *IEEE Transactions on Plasma Science*, Vol. 38, No. 4, 2010, pp. 1052–1057.

[5] N. Koch, H. P. Harmann, and G. Kornfeld, "Development and test status of the THALES high efficiency multistage plasma (HEMP) thruster family," in *Proceedings of the 29th International Electric Propulsion Conference*, IEPC Paper No. 2005–297, Princeton, 2005.

[6] N. A. MacDonald, C. V. Young, M. A. Cappelli, and W. A. Hargus, Jr., "Ion velocity and plasma potential measurements of a cylindrical cusped field thruster," *Journal of Applied Physics*, Vol. 111, 093303, 2012.

[7] S. Harada, T. Baba, A. Uchigashima, S. Yokota, A. Iwakawa, A. Sasoh, T. Yamazaki, and H. Shimizu, "Electrostatic acceleration of helicon plasma using a cusped magnetic field," *Applied Physics Letters*, Vol. 105, 194101, 2014.

[8] D. Ichihara, A. Uchigashima, A. Iwakawa, and A. Sasoh, "Electrostatic ion acceleration across a diverging magnetic field," *Applied Physics Letters*, Vol. 109, 053901, 2016.